Thermal shifts and intermittent linear response of aging systems

Paolo Sibani and Simon Christiansen[*]

Institut for Fysik og Kemi, SDU, DK5230 Odense M, Denmark
(Received 17 December 2007; published 8 April 2008)

At time t after an initial quench, an aging system responds to a perturbation turned on at time $t_w < t$ in a way mainly depending on the number of intermittent energy fluctuations, so-called quakes, which fall within the observation interval (t_w, t) [P. Sibani, G. F. Rodriguez, and G. G. Kenning, Phys. Rev. B **74**, 224407 (2006); P. Sibani, Eur. J. Phys. B **58**, 483 (2007)]. The temporal distribution of the quakes implies a functional dependence of the average response on the ratio t/t_w. Further insight is obtained imposing small temperature steps, so-called T shifts. The average response as a function of $t/t_{w,\text{eff}}$, where $t_{w,\text{eff}}$ is the effective age, is similar to the response of a system aged isothermally at the final temperature. Using an Ising model with plaquette interactions, the applicability of analytic formulas for the average isothermal magnetization is confirmed. The T-shifted aging behavior of the model is approximately described using effective ages. Large positive shifts nearly reset the effective age. Negative T shifts offer a more detailed probe of the dynamics. Assuming the marginal stability of the "current" attractor against thermal noise fluctuations, the scaling form $t_{w,\text{eff}} = t_w^x$ and the dependence of the exponent x on the aging temperatures before and after the shift are theoretically available. The predicted form of x has no adjustable parameters. Both the algebraic scaling of the effective age and the form of the exponent reasonably agree with the data. The present simulations thus confirm the crucial role of marginal stability in glassy relaxation.

I. INTRODUCTION

Rejuvenation, memory, and other intriguing aspects of out-of-equilibrium thermal relaxation, a process widely known as aging, continue to attract experimental and theoretical interest [1–17].

One starting point for theoretical analyses is the real-space morphology of spin-glasses with short-range interactions, where thermalized domains form, with a linear size growing in time as $R(t) \propto t^\lambda$ [6–8,18]. The domain size corresponds to the thermal correlation length and can be extracted from numerical simulation data. Furthermore, the temperature dependence of the exponent λ can be rationalized by assuming that the energy barrier controlling domain growth increases logarithmically in time [8,18]. The same logarithmic time dependence characterizes hierarchical models, which account for, e.g., memory effects and use configuration-space, or "landscape," properties as the starting point [4,19,20]. A third theoretical approach focuses on the relationship between linear response and autocorrelation functions. Numerical [21,22] and experimental [23–25] results show that the fluctuation dissipation theorem (FDT) is applicable for observation times $t_{obs} < t_w$, where t_w is the time at which the perturbation is applied. While the FDT is broken for larger t_{obs}, the proportionality between conjugate response and correlation functions may be restored asymptotically for large t_w and t_{obs}, from which a general description flows in terms of effective temperatures [25–28]. Last but not least, fluctuation spectra [22,29–33] indicate that thermally activated aging processes, linear response functions included, are controlled by intermittent transitions between metastable attractors which irreversibly release the ex-

cess energy trapped in the initial configuration. These events, dubbed quakes, have statistical properties suggesting that they might be triggered by thermal fluctuations of record magnitude [34,35].

Based on the idea that metastable attractors of glassy systems are marginally stable and that the transitions between them are hence induced by record sized thermal fluctuations, a "record dynamics" scenario [36] provides approximate analytical formulas for several physical quantities. The arguments leading to these results ignore quasiequilibrium properties, but are sufficiently general to support the universal character of off-equilibrium aging phenomena [18,34,37–41]. To buttress a comprehensive, albeit approximate, description of nonequilibrium aging based on record dynamics, this paper discusses numerical simulations of an Ising model with plaquette interactions and with a glassy dynamical regime at low temperatures. The work extends numerical investigations [31,32] of the same model and experimental and numerical studies of linear response in spin glasses [22,30].

Aging under isothermal conditions is considered first, and analytic formulas for the average magnetization [22,30] are verified. Second, the effect of "T steps" or "T shifts," small temperature steps of either sign applied concurrently with the magnetic field, is analyzed in terms of *effective ages*. Replacing the system age t_w as a scaling parameter, the effective age makes the average response appear similar to the isothermal response at the final temperature. Effective ages give an excellent parametrization of the average response for negative shifts and a reasonable one for positive shifts. However, even for negative shifts, fluctuation spectra cannot be fully described by an effective age.

For negative T shifts, an algebraic relation between effective and true age exists [17]. The predicted analytical dependence of the corresponding exponent on the temperatures before and after the step has no adjustable parameters. Both

*paolo.sibani@ifk.sdu.dk
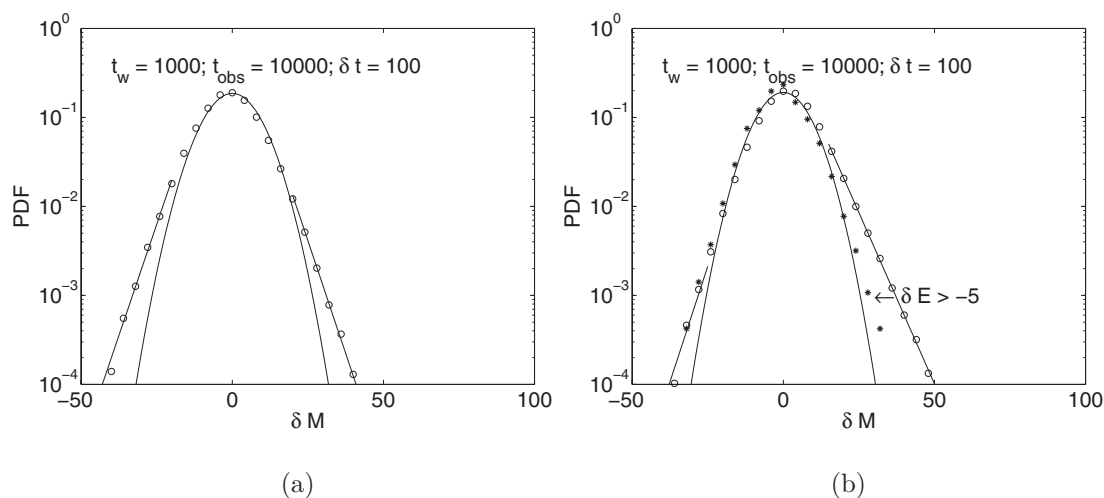
FIG. 1. (a) The PDF of the spontaneous magnetic fluctuations has a Gaussian central part and two symmetric intermittent wings. Data are sampled in the interval $t_w, t_w + t_{obs}$. (b) The same quantity (outer graph) when a field $H = 0.3$ is turned on at $t_w = 1000$. The left intermittent wing is clearly reduced, and the right intermittent wing is amplified. The inner, almost Gaussian shaped, PDF is the *conditional* PDF obtained by excluding the magnetic fluctuations which are synchronous with large and negative energy changes (the quakes)—i.e., energy changes $\delta E < -5$. The lines are fits to a zero centered Gaussian and to two exponentials, which are obtained using different subsets of the data. All simulations are performed isothermally at the temperature $T = 1.5$.

the algebraic scaling and the form of the exponent are confirmed by the present simulations. The final discussion emphasizes the ramified connections of our approach to other descriptions of aging dynamics, focusing in particular on how the general character of the results presented is related to the behavior in the thermodynamic limit of the eigenvalue spectrum of the quake-induced dynamics.

II. MODEL AND METHOD

In spite of its simplicity and, in particular, in spite of its lack of quenched disorder and the triviality of its ground states, the p-spin model has full fledged aging behavior [31,42,43]. In the model, N Ising spins, $\sigma_i = \pm 1$, are placed on a cubic lattice with periodic boundary conditions. They interact through the plaquette Hamiltonian

$$\mathcal{H} = -\sum_{\mathcal{P}_{ijkl}} \sigma_i \sigma_j \sigma_k \sigma_l + H \eta(t_w - t) \sum_i \sigma_i, \qquad (1)$$

where the first sum runs over all the elementary plaquettes of the lattice, including for each plaquette the product of the four spins located at its corners. The second sum describes the coupling of the total magnetization, $\Sigma \sigma_i$, to an external magnetic field. As expressed by the Heaviside step function $\eta(t_w - t)$, the field jumps at $t = t_w$ from zero to a value $H > 0$.

The simulations utilize the waiting time method (WTM) [44], a rejectionless algorithm endowed with an "intrinsic" time unit approximately corresponding to one Monte Carlo sweep. By choosing a high-energy random configuration as initial state for low-temperature isothermal runs, an instantaneous initial thermal quench is effectively achieved. All simulation temperatures are within the model aging regime $0.5 < T < 2.5$. To improve the statistics, probability distribution functions (PDFs) are collected over 2000 independent runs for each set of physical parameters. Other statistical data are collected over 1000 independent runs.

In the following, the symbol t stands for the time elapsed from the initial quench (and from the beginning of the simulations). The field is switched on at time t_w, and data are collected during the "observation" time $t_{obs} = t - t_w$. The external field jumps from zero to $H = 0.3$ at $t = t_w$. The thermal energy is denoted by E, the magnetization by M, and the respective fluctuations by δE and δM. The latter are calculated as finite time differences over time intervals of length $\delta t \ll t_{obs}$. The average magnetization per spin is denoted by μ_{ZFCM}.

III. RESULTS

The statistical subordination to the quakes of intermittent physical changes occurring in an aging process [22,30,40,45] is the crucial element of a record dynamics description. For completeness, we therefore include recent supporting evidence [32] related to the present model.

The circles in Fig. 1 (see Ref. [32]) show, on a logarithmic vertical scale, PDFs of the magnetic fluctuations δM in the interval $[t_w, t_w + t_{obs}]$. The data in the left panel are spontaneous magnetic fluctuations (no field), while those in the right panel are effected by an external magnetic field switched on at $t = t_w = 1000$. In both panels, intermittent wings extend a zero-centered central Gaussian spectrum. The magnetic field enhances the positive wing, reduces the negative wing, and leaves the Gaussian spectrum unchanged. In the right panel, a conditional PDF (stars) is also shown. The PDF is obtained by removing from the statistics all magnetic fluctuations occurring within the same or the next interval of duration δt as energy fluctuations of magnitude $\delta E \leq -5$. As the threshold chosen demarcates the onset of the intermittent behavior of the heat flow PDF [32], the filtering removes the magnetic fluctuations concurrent with the quakes. Since the resulting conditional PDF is nearly Gaussian, the intermittent
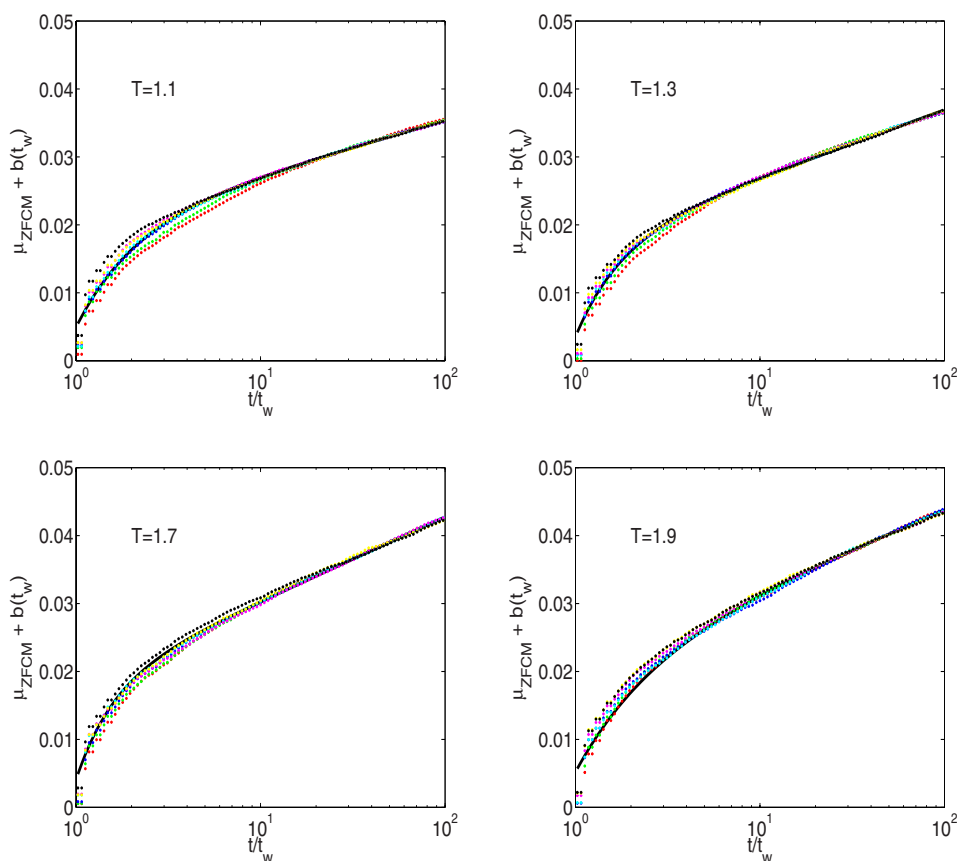
FIG. 2. (Color online) For each temperature indicated, the four panels depict scaling plots of the average magnetization per spin, vertically adjusted by the constant $b(t_w)$. The values of t range from $t=t_w$ to $400t_w$, with $t_w=50$, 100, 200, 500, and 1000, (circles). The (black) line is a fit to Eq. (3).

magnetic fluctuations carrying the average magnetic response are all closely associated with the quakes. Furthermore, the energy and, in particular, the quakes are hardly affected by the magnetic field. Therefore, the quakes dissipate the excess energy entrapped in the initial (zero-field) configuration [31,32] and the field probes but does not modify the spontaneous intermittent dynamics.

As argued in Ref. [36], the number of quakes in the interval (t,t') is theoretically described by a Poisson distribution with average

$$n_I(t',t) = \alpha(N)\ln(t/t').$$ (2)

In theory, $\alpha(N)$ depends linearly on the system size N and not at all on temperature. The present model has nearly the same behavior [32].

A. Isothermal aging

The assumption that a physical processes is subordinated to statistically independent quakes neglects, e.g., the dynamical effects of equilibriumlike fluctuations, and the results are therefore inherently approximate, yet simple and reasonably accurate. From the assumption it follows that the number n of quakes falling in a given observation interval assumes the same dynamical role as the time variable in a homogeneous Markov process. The n dependent moments of this process describe physical observables and admit eigenvalue expansions. Averaged over the Poisson distribution of n, the expansions produce expressions for the moments [22,30,45] which feature the ratio t/t_w between the end-points t_w and t

of the observation interval as a scaling variable. For reasons discussed later, expressions truncated after a few leading terms are usually satisfactory. E.g., the average linear response of the p-spin model is well approximated by

$$\mu_{\text{ZFCM}} = b_0 + a_m \ln\left(\frac{t}{t_w}\right) + b_m\left(\frac{t}{t_w}\right)^{\lambda_m},$$ (3)

where b_0, a_m, b_m, and λ_m are parameters. The exponent λ_m is negative, from which, asymptotically, the behavior becomes logarithmic. Figure 2 shows the average linear response versus t/t_w for the temperatures indicated in the four plots. Each plot displays data sets (dots) for $t_w=100$, 200, 400, 600, 800, 1000, and 2000. The solid line is a fit to Eq. (3). In order to include the stationary contribution to the magnetization, which is ignored in the theory, the constant b_0 in Eq. (3) is modified by an additive t_w-dependent term. The correction increases with t_w, but stays within a few percent of the total. The black line is obtained by fitting to Eq. (3). For the smallest values of the abscissa, the quality of the data collapse, and consequently, of the fit, is higher the higher the temperature. For larger values of the abscissa, all fits are equally satisfactory. In summary, the isothermal aging behavior is rather well described by Eq. (3). The deviations from t/t_w scaling are due to the discreteness of the spectrum of available energies, which becomes more important for lower temperatures [32].

B. Effect of T shifts

The response function of spin glasses [8,46] is systematically affected by a small temperature change, a so-called T
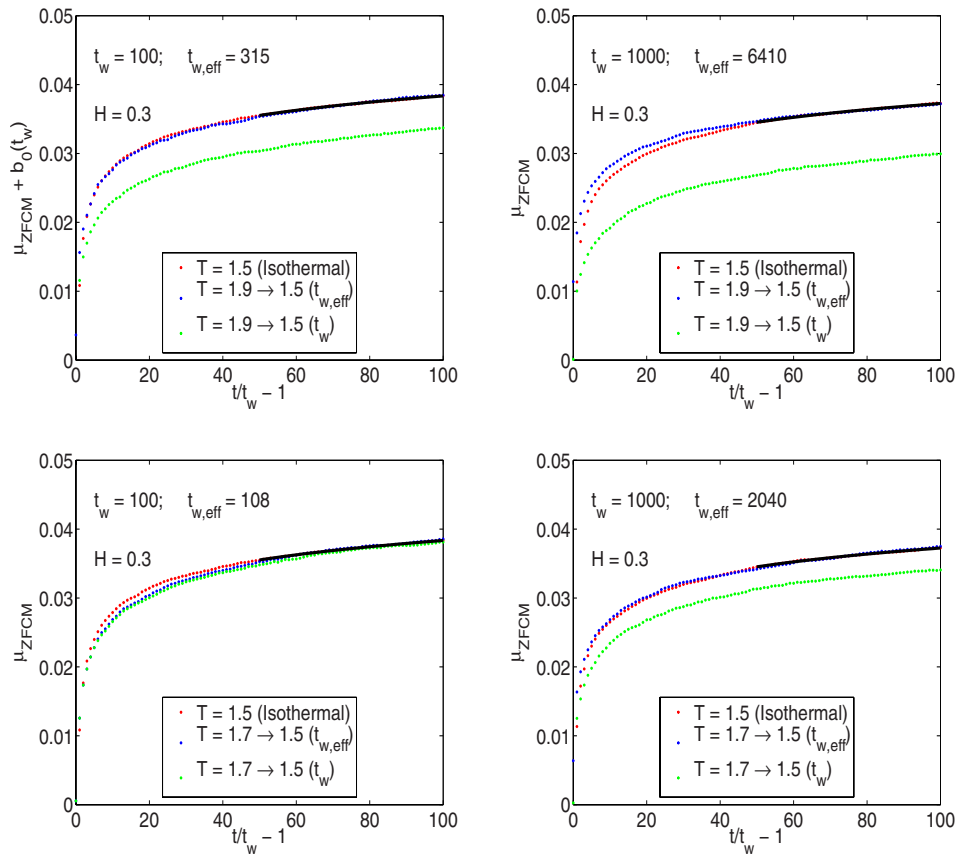
FIG. 3. (Color online) For the temperatures indicated, the four panels depict scaling plots of the average magnetization per spin, shifted by the constant $b_0(t_w)$. In each panel, three sets of data are shown. The ordinate is the average linear response under different conditions. The abscissa is, apart from an additive constant, the system age t, scaled with either the true or the effective age. The two nearly overlapping data sets are for (i) isothermal response at the indicated temperature, versus the age scaled by t_w, and (ii) T-shifted response, plotted versus the system age scaled by $t_{w,\text{eff}}$. The quality of the collapse of these two data sets gauges the relevance of the effective age parametrization. (iii) Same data as (ii), but using the actual t_w value to scale the age.

shift, applied during the aging process, usually together with a field switch at age t_w. E.g., as a function of t_{obs}, the logarithmic derivative $S(t_w, t_{\text{obs}})$ of the average magnetization peaks at $t_{\text{obs}} = t_w$ under isothermal conditions. The peak moves to a lower (higher) value when positive (negative) temperature shifts are applied. As the same effect can be achieved isothermally at the final temperature using a shorter, respectively longer t_w, an effective age $t_{w,\text{eff}}$ expectedly provides a natural and general parametrization of the data. A previous study of the intermittent heat transfer of the Edward-Andersen spin-glass model [17] under a T shift and the present study both confirm and to a certain extent qualify this conclusion.

Below, we consider how both negative and positive T shifts affect the average response function of the plaquette model. We furthermore discuss how negative shifts affect the spectrum of intermittent magnetization fluctuations. Figure 3 shows the average magnetic response, vertically adjusted by a small t_w-dependent term, as previously discussed, for a negative T shift imposed concurrently with the field switch at t_w. Each panel of Fig. 3 contains three curves. In the lowest curve the T-shifted magnetization is plotted versus the scaling variable $t/t_w - 1$. The two, nearly overlapping, and higher lying, curves are (i) the T-shifted data again, now plotted

versus $t/t_{w,\text{eff}} - 1$, with $t_{w,\text{eff}}$ chosen to maximize the data collapse, and (ii) isothermal magnetization at the final temperature, plotted versus $t/t_w - 1$. Clearly, scaling by a suitable effective age accounts rather well for the average linear response following a negative T shift. Figure 4 is similar to Fig. 3, except that the applied T shifts are now positive. In each panel, the highest-lying curve shows the T-shifted magnetization versus $t/t_w - 1$. The two lower lying curves are (i) the T-shifted magnetization data, now plotted versus $t/t_{w,\text{eff}} - 1$, and (ii) the magnetization curve obtained for isothermal aging at the final temperature, plotted versus $t/t_w - 1$. Note that the transient effects produced by a positive shift are not fully described by an effective age. Consequently, the "best" value of $t_{w,\text{eff}}$ is obtained by a fit which only maximizes data overlap for large t/t_w values.

Figure 4 shows that positive T shifts lead, as expected, to effective ages smaller than the actual ages. The best achievable data collapse is not as good as for negative shifts, especially for small values of t/t_w. Since a positive T shift destroys, totally or in part, the current configuration, it clearly induces additional dynamical effects not well represented by an effective age. Yet the numerical results for positive shifts qualitatively concur with a crucial hypothesis of record dynamics: namely, that the attractors successively visited are all
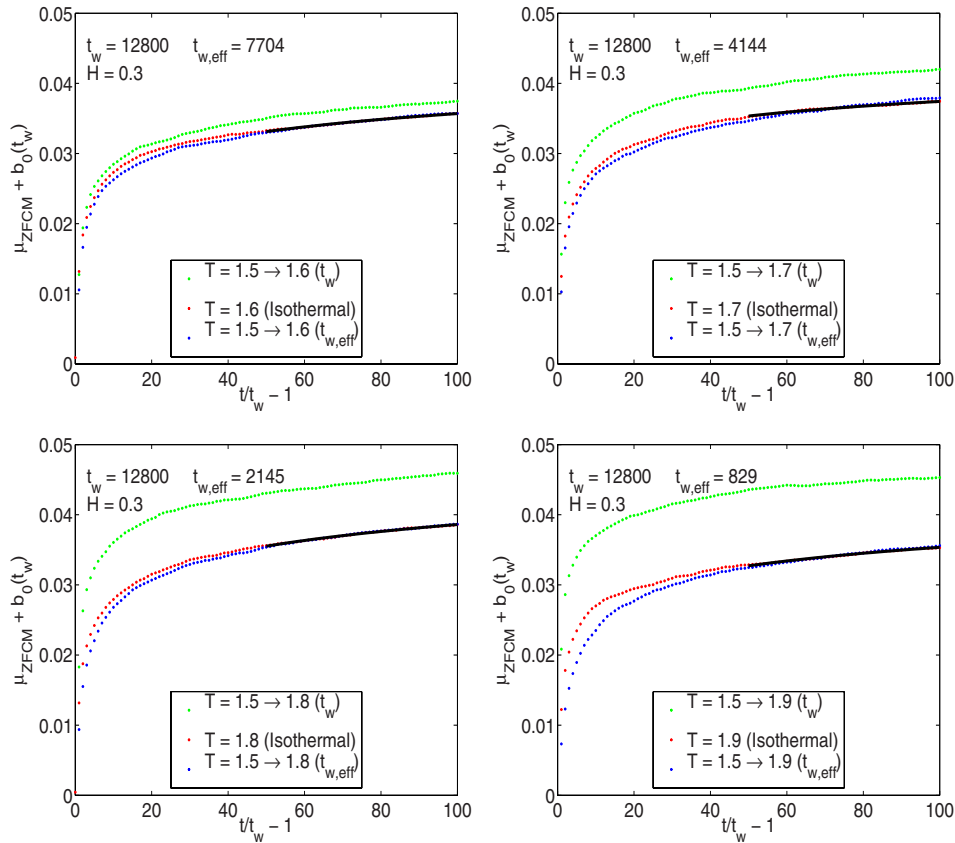
FIG. 4. (Color online) The four panels depict, for the temperatures indicated, scaling plots of the average magnetization per spin, vertically adjusted by the constant $b_0(t_w)$. In each panel, three sets of data are shown. The ordinate is the average linear response under different conditions. The abscissa is, apart from an additive constant, the system age t, scaled with either the true or the effective age. The two nearly overlapping data sets are (i) isothermal response at the given temperature, versus the age scaled by t_w, and (ii) T shifted response. The data are plotted versus the age scaled by $t_{w,\mathrm{eff}}$. The quality of the collapse of the first two data sets gauges the relevance of the effective age parametrization. (iii) Same data as (ii), but using the actual t_w value to scale the age.

marginally stable; i.e., they are destabilized by a record sized thermal fluctuation. Increasing the temperature leads to larger thermal fluctuations and hence to the destruction of the configuration reached at t_w. Negative shifts have more subtle consequences, which yield to an analytical description. We first consider how negative shifts affect the spectrum of the magnetization fluctuations. Second, the algebraic relationship between true and effective age is explained theoretically and checked against simulation data.

A system undergoing a negative T shift $T=1.9 \rightarrow T=1.5$ at $t_w=1000$ has, according to Fig. 3, second panel, an effective age $t_{w,\mathrm{eff}} \approx 6400$. If its dynamics were fully equivalent to the isothermal dynamics of a system of age $t_{w,\mathrm{eff}} \approx 6400$, the PDFs of magnetization differences δM calculated over intervals of the same length δt would overlap in the two cases. In Fig. 5, the PDF of isothermal fluctuations for a system with $t_w=6400$ (stars) is compared to the corresponding PDF of a T-shifted system of age $t_w=1000$ (circles). Both data sets are plotted on a logarithmic vertical scale. The Gaussian parts overlap, but the intermittent tails do not. The tails are however parallel, meaning that the weight of the intermittent fluctuations relative to the weight of the Gaussian fluctuations is higher in the T-shifted case, even though the normalized size distribution of the intermittent fluctuations has the
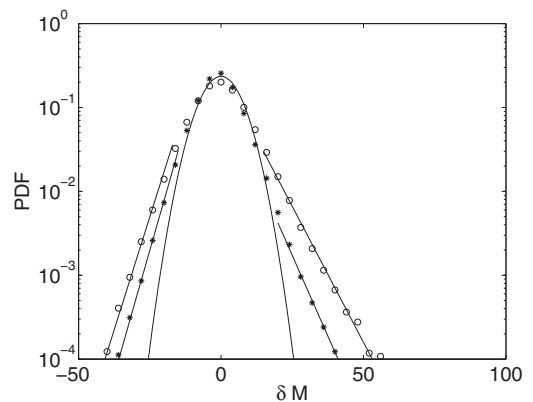
FIG. 5. The PDF of magnetic fluctuations for isothermal (stars) and T-shifted (circles) protocols. The data are collected in intervals of type $[t, 50t]$. The initial ages are $t_{w,\mathrm{eff}}=6400$ for isothermal aging and $t_w=1000$ for T-shifted aging. The δM values are calculated over intervals of size $\delta t=500$. A full collapse would imply the full equivalence of the T-shifted response and the isothermal response of a system of the correct effective age. The lines are fits to a zero centered Gaussian and to two exponentials, which are obtained using different subsets of the data.
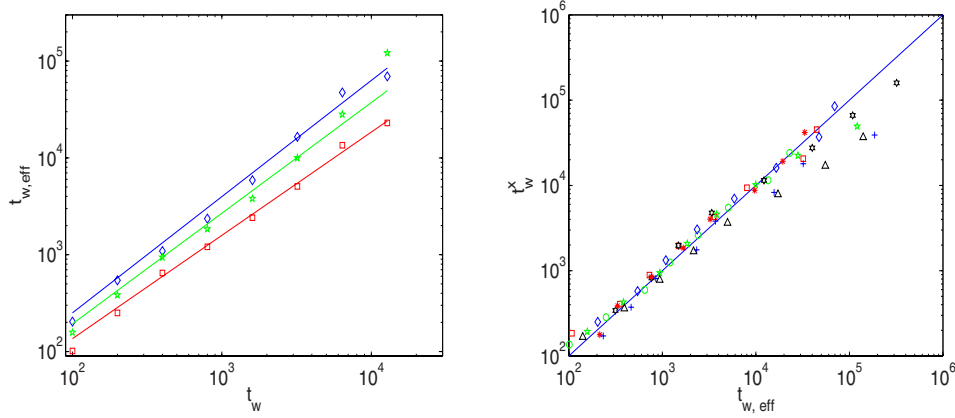
FIG. 6. (Color online) The left panel shows the algebraic relation between the effective and the actual age for the three different T shifts $1.6 \rightarrow 1.5$ (red squares), $1.8 \rightarrow 1.5$ (green polygons), and $1.6 \rightarrow 1.4$ (blue diamonds). Other cases analyzed are not shown for graphical reasons The solid lines correspond to the analytical prediction $t_{w,eff} = t_w^x$, where x is determined by a least square fit. In the right panel, t_w^x is plotted versus $t_{w,eff}$ using different symbols and colors for all available x values. Deviations from the line gauge the discrepancy between predicted and observed behavior.

same shape in both cases. However, since the Gaussian fluctuations have zero average, the average response is described via $t_{w,eff}$, precisely as previously discussed.

In a record dynamics scenario, the marginally stable attractor reached at t_w is associated to a dynamical barrier of magnitude $b(t_w)$, which matches the largest among the thermal energy fluctuations experienced by the system through the aging process up to age t_w. This barrier grows with the system age in a logarithmic fashion, as explained below. Note that the arguments used implicitly require that the dynamics have access to a continuum of barriers and hence to a continuum of energy values. For Ising models in particular, the granularity of the energy spectrum becomes important at low temperatures and some deviation from the predicted behavior can be expected, as noted already.

Thermal fluctuations are described by the equilibrium Boltzmann distribution $P(E)$ characterizing a single thermalized domain. In our case, the local density of states can be considered constant, from which $P(E) \propto \exp(-E/T)$. If we assume that the shape of $P(E)$ remains the same for all metastable attractors visited, a jump from one attractor to the next is induced by a thermal fluctuations of record size drawn from the distribution $P(E)$. At time t_w, the largest energy fluctuation ever impinging on the system will be the largest among a number of order t_w of equilibrium fluctuations at temperature T. Due to the form of $P(E)$, the magnitude of the extremal barrier scales as $b(t_w) \propto T \ln(t_w)$ [17]. Note that the scaling follows from the extremality of the barrier, not from standard kinetic considerations related to thermal relaxation. Yet the Arrhenius escape time corresponding to $b(t_w)$ equals t_w. Hence, at constant temperature sufficient time is available to thermalize in the current metastable region of configuration space, before a record fluctuation pushes the system into a different configuration.[1] A negative T shift from T_i to $T_f < T_i$ effectively rescales the dynamical barrier to $b(t_w)T_i/T_f$,

and the corresponding Arrhenius time becomes $t_{w,eff} = \exp[b(t_w)T_i/T_f] = t_w^{T_i/T_f}$. We thus conclude that

$$t_{w,eff} = t_w^{x(T_i, T_f)}, \quad x(T_i, T_f) = \frac{T_i}{T_f}. \quad (4)$$

In summary, the algebraic relationship between effective and true age flows from the logarithmic time growth of the dynamical barrier which, in the present theory, is a consequence of its extremal character. The temperature dependence of the exponent x given above has no adjustable parameters. In Fig. 6, left panel, the empirically determined effective age is plotted versus the actual age on a log-log scale for T shifts $1.6 \rightarrow 1.5$ (red squares) $1.8 \rightarrow 1.5$ (green polygons), and $1.6 \rightarrow 1.4$ (blue diamonds). The slopes of the corresponding lines, which are obtained by linear regression, provide a numerical estimate of the values of the exponent x. Several other T shifts are also considered, but the corresponding data are not shown for graphical reasons. The values of t_w^x corresponding to all available x values are plotted versus the empirical effective age in the right panel of Fig. 6. The color and symbol coding is as follows: $1.6 \rightarrow 1.5$ (circles), $1.7 \rightarrow 1.5$ (squares), $1.8 \rightarrow 1.5$ (diamonds) $1.9 \rightarrow 1.5$ (hexagons), $1.6 \rightarrow 1.4$ (polygons), $1.8 \rightarrow 1.6$ (stars), $1.8 \rightarrow 1.6$ (plusses), and $2.0 \rightarrow 1.8$, (upper triangles). The solid line embodies the theoretical prediction given in Eq. (4). Thus, the distance between the points and the line represents the mismatch between data and theory. Except for shifts involving a relatively high initial temperature, especially for high values of the effective age, the agreement is satisfactory.

IV. DISCUSSION

References [22,30,40,45] have argued that using the number of quakes, n, as an effective "time" variable produces a

---

[1]In the Edward-Andersen spin-glass model, the local equilibrium distribution and the exponent x are affected by an exponentially growing local density of states $\mathcal{D}(E) \propto \exp(E/\epsilon)$. In the present model the local density of state has no important energy dependence.

translationally invariant reparametrized aging description which is generic, albeit approximate. The stochastic changes induced by the quakes can either be dealt with by further modeling assumptions [40,45] or by using generic eigenvalue expansions of the averages as a function of n [30]. Averaging these expansions over the Poisson distribution of n turns each exponential term—e.g., ae^{cn}—of the eigenfunction expansion into a fractional power $a(t/t_w)^{\lambda_c}$. By simple algebra, the exponent λ_c corresponding to a given eigenvalue c of the time reparametrized problem is given by

$$\lambda_c(T,N) = \alpha(N)(e^{c(N,T)} - 1), \quad (5)$$

where the dependence on the system size N and temperature T is now explicitly introduced. In summary, the eigenvalue expansion leads to a generic, but from the outset highly parametrized, description of aging dynamics. Fortunately, as discussed below, for large values of the system size N only a few parameters remain dynamically relevant and physically meaningful.

In the following, the symbol λ_c denotes a generic exponent not to be confused with the (nearly) homonymous dynamical exponent λ widely used in the literature. We expect that all exponents $c(N,T)$ of the time homogeneous reparametrized dynamics be negative or zero, as usual for relaxational dynamics. Since α is always positive, the same property is shared by λ_c. Due to the extensivity of the number of thermalized domains, $\alpha(N) \propto N$. The following three possibilities arise for the exponent λ_c in the limit $N \to \infty$: (i) $\lambda_c(T,N) \to -\infty$. In this case, the corresponding expansion term is irrelevant as it quickly decays to zero. This behavior occurs whenever $c(N,T)$ remains bounded away from zero in the thermodynamic limit. (ii) $\lambda_c(T,N) \to 0$. In this case the corresponding expansion term is frozen and can be included into a constant term. This behavior occurs whenever $c(N,T)$ approaches zero *faster* than $1/N$ in the thermodynamic limit. (iii) $\lambda_c(T,N)$ remains finite and bounded away from zero. In this case the corresponding expansion term is dynamically relevant. This behavior occurs when $c(N)$ vanishes in the thermodynamical limit in proportion to $1/N$. Observable power laws are thus only connected to the relaxation "time" scales of the reparametrized dynamical problem which diverge linearly with system size; see, e.g., Ref. [45] for an explicit demonstration. The corresponding exponents have the form $\lambda_c(T) = \alpha(N)c(N,T)$, a form which is asymptotically independent of N for large N.

Far away from equilibrium (and hence from saturation), the smallest relevant exponent can be small enough to justify the further expansion $(t/t_w)^{\lambda_c} \propto 1 + \lambda_c \ln(t/t_w)$ for a wide range of t/t_w. Whenever a logarithmic time dependence exists, it is dominant for large values of t/t_w. This widely observed logarithmic behavior implies that linear response and autocorrelation are (asymptotically) proportional as in thermal equilibrium, but for rather different reasons. An effective temperature can be defined, albeit in a nonuniversal manner [28], via the fluctuation dissipation ratio.

Numerical studies of domain growth convincingly show that the characteristic linear size of a thermalized domain increases algebraically in time [8,18]. In that context, the T dependence of the growth exponent λ indicates that the energy barrier surmounted at age t grows logarithmically with t. The explanation appears, however, to be *ad hoc* and differs from the original assumption of Fisher and Huse [47], who expected a power-law scaling. In record dynamics, the logarithmic time increase of the dynamical barrier flows directly from the proportionality between said barrier and the typical size of the extremal energy fluctuation at age t. The logarithmic barrier growth leads then to the temperature dependence of the exponent x given in Eq. (4). Even though the linear domain size $R(t)$ does not appear conspicuously in the present description, the latter definitely attributes central dynamical features to the presence of localized and noninteracting domains—e.g., the linear system size dependence of the factor α. A hierarchical energy landscape is attached to each domain [34,49]: In such landscape energy fluctuations of record size are, by construction, needed to trigger a change of metastable attractor. Hierarchical structures are most usually associated to mean-field models, whose equilibrium free-energy landscapes have ultrametric properties [48]. By contrast, hierarchies are here defined purely in terms of dynamical barriers and their corresponding time scales [34,49]. Mean-field concepts are widely used in the literature. e.g., recently to describe the response of mesoscopic systems [50]. Establishing a theoretical connection to this type of approach is an interesting open problem.

In conclusion, we have analyzed a simple but typical aging system with no quenched disorder. To the extent the present results can be generalized as expected, a simple record dynamics description can approximately account for (i) the linear response phenomenology, including the effect of temperature shifts; (ii) the origin of asymptotic descriptions in term of effective temperatures; and (iii) the interplay of real space properties—i.e., domains—and hierarchical properties associated with the energy landscape of each domain.

[1] L. Lundgren, P. Nordblad, and L. Sandlund, Europhys. Lett. **1**, 529 (1986).

[2] C. Schulze, K. H. Hoffmann, and P. Sibani, Europhys. Lett. **15**, 361 (1991).

[3] P. Sibani and K. H. Hoffmann, Europhys. Lett. **16**, 423 (1991).

[4] K. H. Hoffmann, S. Schubert, and P. Sibani, Europhys. Lett. **38**, 613 (1997).

[5] K. Jonason, E. Vincent, J. Hammann, J. P. Bouchaud, and P. Nordblad, Phys. Rev. Lett. **81**, 3243 (1998).

[6] T. Komori, H. Yoshino, and H. Takayama, J. Phys. Soc. Jpn. **68**, 3387 (1999).

[7] T. Komori, H. Yoshino, and H. Takayama, J. Phys. Soc. Jpn. **69**, 1192 (2000).

[8] H. Yoshino, T. Komori, and H. Takayama, J. Phys. Soc. Jpn. **69**, 228 (2000).

[9] Valéry Normand, Stéphane Muller, Jean-Claude Ravey, and Alan Parker, Macromolecules **33**, 1063 (2000).

[10] M. Utz, P. G. Debenedetti, and F. H. Stillinger, Phys. Rev. Lett. **84**, 1471 (2000).

[11] Jean-Philippe Bouchaud, Vincent Dupuis, Jacques Hammann, and Eric Vincent, Phys. Rev. B **65**, 024439 (2001).

[12] Mario Nicodemi and Henrik Jeldtoft Jensen, J. Phys. A **34**, 8425 (2001).

[13] D. Bonn, S. Tanase, B. Abou, H. Tanaka, and J. Meunier, Phys. Rev. Lett. **89**, 015701 (2002).

[14] Ludovic Berthier and Jean-Philippe Bouchaud, Phys. Rev. B **66**, 054404 (2002).

[15] Hajime Takayama and Koji Hukushima, J. Phys. Soc. Jpn. **71**, 3003 (2002).

[16] H. J. Jensen and M. Nicodemi, Europhys. Lett. **57**, 348 (2002).

[17] Paolo Sibani and Henrik Jeldtoft Jensen, J. Stat. Mech.: Theory Exp. (2004) P10013.

[18] H. Rieger, J. Phys. A **26**, L615 (1993).

[19] E. Vincent, in *Recent Progress in Random Magnets*, edited by D. H. Ryan (McGill University, Montreal, 1991), pp. 209–246.

[20] V. Dupuis, E. Vincent, J.-P. Bouchaud, J. Hammann, A. Ito, and H. Aruga Katori, Phys. Rev. B **64**, 174204 (2001).

[21] J.-O. Andersson, J. Mattsson, and P. Svedlindh, Phys. Rev. B **46**, 8297 (1992).

[22] P. Sibani, Eur. Phys. J. B **58**, 483 (2007).

[23] P. Svedlindh, K. Gunnarsson, P. Nordblad, L. Lundgren, H. Aruga, and A. Ito, Phys. Rev. B **40**, 7162 (1989).

[24] D. Hérisson and M. Ocio, Phys. Rev. Lett. **88**, 257202 (2002).

[25] L. Buisson, L. Bellon, and S. Ciliberto, J. Phys.: Condens. Matter **15**, S1163 (2003).

[26] Leticia F. Cugliandolo, Jorge Kurchan, and Luca Peliti, Phys. Rev. E **55**, 3898 (1997).

[27] Horacio E. Castillo, Claudio Chamon, Leticia F. Cugliandolo, José Luis Iguain, and Malcom P. Kenneth, Phys. Rev. B **68**, 134442 (2003).

[28] Pasquale Calabrese and Andrea Gambassi, J. Phys. A **38**, R133 (2005).

[29] P. Sibani and H. Jeldtoft Jensen, Europhys. Lett. **69**, 563 (2005).

[30] P. Sibani, G. F. Rodriquez, and G. G. Kenning, Phys. Rev. B **74**, 224407 (2006).

[31] P. Sibani, Phys. Rev. E **74**, 031115 (2006).

[32] S. Christiansen and P. Sibani, New J. Phys. **10**, 033013 (2008).

[33] A. Crisanti and F. Ritort, Europhys. Lett. **66**, 253 (2004).

[34] P. Sibani, C. Schön, P. Salamon, and J.-O. Andersson, Europhys. Lett. **22**, 479 (1993).

[35] P. Sibani and B. Peter, Phys. Rev. Lett. **71**, 1482 (1993).

[36] Paolo Sibani and Jesper Dall, Europhys. Lett. **64**, 8 (2003).

[37] Luca Cipelletti, S. Manley, R. C. Ball, and D. A. Weitz, Phys. Rev. Lett. **84**, 2275 (2000).

[38] Christophe Josserand, Alexei V. Tkachenko, Daniel M. Mueth, and Heinrich M. Jaeger, Phys. Rev. Lett. **85**, 3632 (2000).

[39] A. Hannemann, J. C. Schön, M. Jansen, and P. Sibani, J. Phys. Chem. B **109**, 11770 (2005).

[40] L. P. Oliveira, Henrik Jeldtoft Jensen, Mario Nicodemi, and Paolo Sibani, Phys. Rev. B **71**, 104526 (2005).

[41] Paul Anderson, Henrik Jeldtoft Jensen, L. P. Oliveira, and Paolo Sibani, Complexity **10**, 49 (2004).

[42] A. Lipowski and D. Johnston, Phys. Rev. E **61**, 6375 (2000).

[43] M. R. Swift, H. Bokil, R. D. M. Travasso, and A. J. Bray, Phys. Rev. B **62**, 11494 (2000).

[44] Jesper Dall and Paolo Sibani, Comput. Phys. Commun. **141**, 260 (2001).

[45] Paolo Sibani, Europhys. Lett. **73**, 69 (2006).

[46] P. Granberg, L. Sandlund, P. Nordblad, P. Svedlindh, and L. Lundgren, Phys. Rev. B **38**, 7097 (1988).

[47] D. S. Fisher and D. A. Huse, Phys. Rev. B **38**, 386 (1988).

[48] K. H. Fischer and J. A. Hertz, *Spin Glasses* (Cambridge University Press, Cambridge, England, 1991).

[49] P. Sibani and P. Schriver, Phys. Rev. B **49**, 6667 (1994).

[50] H. Yoshino and T. Rizzo, J. Phys.: Condens. Matter **19**, 145223 (2007).